Available online at www.sciencedirect.com

ScienceDirect

Current Opinion in Electrochemistry

Review Article

Insights into electrode–electrolyte interfaces by *in situ* scanning tunnelling microscopy

Maren-Kathrin Heubach[1,a], Yannick Mattausch[1,a] and Timo Jacob[1,2,3]

Fundamental insights into electrode–electrolyte interfaces are crucial for our understanding of electrochemical processes. Standard electrochemical methods, such as cyclic voltammetry, can reveal important information about the systems of interest. Nevertheless, information about structure and morphology of the electrode–electrolyte interface is not that easily accessible. *In situ* scanning tunnelling microscopy can resolve the electrode as well as the direct interface to the electrolyte in real time during electrochemical measurements. This includes changes of the electrode in the nanometre to micrometre range, for example, during metal deposition or corrosion, as well as the observation of ordered molecular adlayers on the electrode. In this work, we want to highlight the capabilities of such studies to better understand the fundamental processes of electrocatalysis and metal deposition and dissolution, which are essential to electrochemical energy storage systems.

Addresses
[1] Institute of Electrochemistry, Ulm University, Albert-Einstein-Allee 47, 89081 Ulm, Germany
[2] Helmholtz-Institute-Ulm (HIU) Electrochemical Energy Storage, Helmholtzstr. 11, 89081 Ulm, Germany
[3] Karlsruhe Institute of Technology (KIT), P.O. Box 3640, 76021 Karlsruhe, Germany

Corresponding author: Jacob, Timo (nawi.ec@uni-ulm.de)
[a] These authors contributed equally to this work.

Current Opinion in Electrochemistry 2024, **48**:101580

This review comes from a themed issue on **Innovative Methods in Electrochemistry (2024)**

Edited by **Bing-Wei Mao** and **Christine Kranz**

For a complete overview see the Issue and the Editorial

Available online xxx

https://doi.org/10.1016/j.coelec.2024.101580

In situ scanning tunnelling microscopy

Since the scanning tunnelling microscope was invented by Binnig and Rohrer in 1982 [1], researchers had the wish to also apply this method in an electrochemical environment to explore electrode–electrolyte interfaces. This was achieved by Itaya and Tomita, who showed the first *in situ* scanning tunnelling microscopy (STM) measurement only a few years later [2]. Two basic requirements must be fulfilled to be able to conduct STM measurements in an electrochemical cell. First, the voltage between the STM tip and the working electrode (WE) as well as the voltage between the WE and the reference electrode (RE) must be controlled separately. This is realised by using a bipotentiostat [3]. Second, the STM tip must be shielded from the electrolyte to prevent Faradaic reactions. Here, different non-conductive coatings can be used, ranging from nail polish to electrophoretic paintings, Apiezon wax, and polyethene [4]. The general experimental setup has not changed much since the first *in situ* or electrochemical STM measurements. Figure 1a shows a schematic drawing of the basic *in situ* STM setup. The WE is placed on the bottom, and the cell compartment with the electrolyte, which is for simplicity not shown here, is mounted on top. RE and counter electrode (CE) are dipped in the electrolyte from aside. A piezoelectric tube scanner enables either movement of the STM tip or the cell. Since the setup needs to be very small, usual cells have a volume of 150–400 µL. Therefore, the CE and RE must be small, often achieved by noble metal wires or microelectrodes [4,5]. Regarding the STM tips, various metals can be used. Nevertheless, *in situ* STM measurements are restricted to wires that are stable against the electrolyte at the respective potentials used. Therefore, metal wires of Pt/Ir alloys are often used, which are rigid and have good electrochemical stability. The tips can either be produced by sophisticated cutting of a wire or by electrochemical etching [6,7]. Figure 1b shows a Pt/Ir (80:20) tip that was electrochemically etched in a NaCN solution. Note that during the etching process, HCN is formed, making a well-ventilated fume hood compulsory. Nevertheless, this etching procedure is capable of reproducibly yielding atomically sharp tips, which are well suited and a prerequisite for atomically resolved imaging. The choice of the tip coating is highly dependent on the used electrolyte and its chemical stability. For example, Figure 1c shows a high-density polyethylene-coated Pt/Ir-tip.

Figure 1

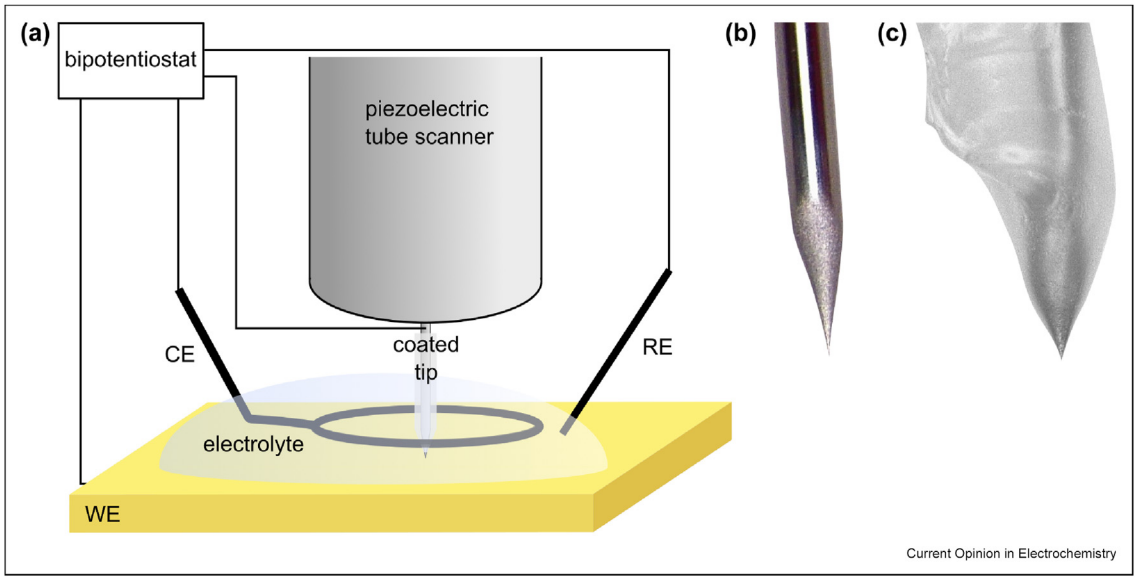

a) Schematic drawing of the typical *in situ* STM setup, **(b)** uncoated STM tip, and **(c)** STM tip coated with high-density polyethylene.

It should be noted that STM images always represent a map of the tunnelling current between the sample surface and the STM tip, thus resembling the electronic nature of the sample. This implies that the tip's geometry may significantly influence the obtained current response (and thus the image) due to tip convolution effects [8,9]. Additionally, even if the STM tips are perfectly shaped and well coated, they could influence the obtained image, for instance, by disrupting adsorption layers, moving deposited material over the surface or leading to preferential deposition or dissolution due to local changes in the electric field around the tip [10]. These aspects always have to be taken into consideration when performing and analysing (*in situ*) STM experiments.

Electrode surface stability

Surface oxidation and corrosion

A fundamental understanding of surface oxidation and corrosion plays an important role in several disciplines of electrochemistry. For instance, in electrocatalysis, formed surface oxides are often the catalytically active sites [11]. Hence, their morphology can significantly influence the electrocatalyst's performance. Thus, by using *in situ* STM in conjunction with other techniques and theoretical simulations, the morphologies of several surface oxides, such as the oxides of Cu [12] or Au [13], could be resolved.

Understanding the initial stages of corrosion is of great interest for corrosion protection. Here again, *in situ* STM can help determine active sites and could provide insights into self-protection mechanisms [14]. It could be shown that grain boundaries and atomic defects are the active sites for corrosion, and three-dimensional oxide growth starts from a two-dimensional hydroxide overlayer, which is adsorbed on the surface [14].

Another corrosion process occurs when, for instance, noble metals are treated at highly positive or highly negative potentials in concentrated electrolytes. This process is known as cathodic corrosion and has been investigated in detail recently [15,16]. Analysis of the cathodic corrosion process by *in situ* STM was performed in an alkaline electrolyte or ionic liquids (ILs) on Ag and Au electrodes [17–19]. It could be determined that the cathodic corrosion of Ag is faster in alkaline electrolytes than in IL-based electrolytes [19] and that cathodic corrosion of Au(111) in an IL starts at the elbow sites of the reconstructed surface [18].

Surface reconstruction

Even between the potentials at which the electrode is reduced or oxidised, the system should not be considered morphologically stable. In particular, Au surfaces undergo surface reconstruction at negative potentials [22]. At the reconstructed surface, the positions of surface atoms deviate from the bulk-truncated configuration due to broken symmetry and broken bonds [23].

In an electrochemical environment, the reconstructed surfaces tend to be stable at potentials negative to the potential of zero charge (*pzc*). A negative surface charge encourages the reconstruction of a surface, while anion

adsorption at positive surface charges induces the lifting of reconstruction, leading to the dominance of an unreconstructed surface [24]. When applying a potential negative of the *pzc* to an already unreconstructed surface, a potential-induced surface reconstruction can be observed [21,22,24]. The surface reconstruction significantly influences the reactivity of the electrode and its activity as an electrocatalyst. Furthermore, the kinetics of the lifting and potential-induced formation of the reconstruction provide information about the mobility of the surface atoms at the applied potential [21,20].

For example, the influence of the applied potential on the surface reconstruction of Au(111) in 0.1 M aqueous H_2SO_4 within the double-layer region is shown in Figure 2a–g [20,21]. After flame-annealing and immersion at −0.6 V *versus* mercury-mercurous sulphate electrode (MSE), the thermally reconstructed Au (111) surface is observed, showing the well-known $(22 \times \sqrt{3})$ periodicity usually referred to as herringbone reconstruction (see Figure 2a) [20]. Stepping the potential to values positive of the *pzc*, such as 0.1 V, leads to the lifting of surface reconstruction in conjunction with the

Figure 2

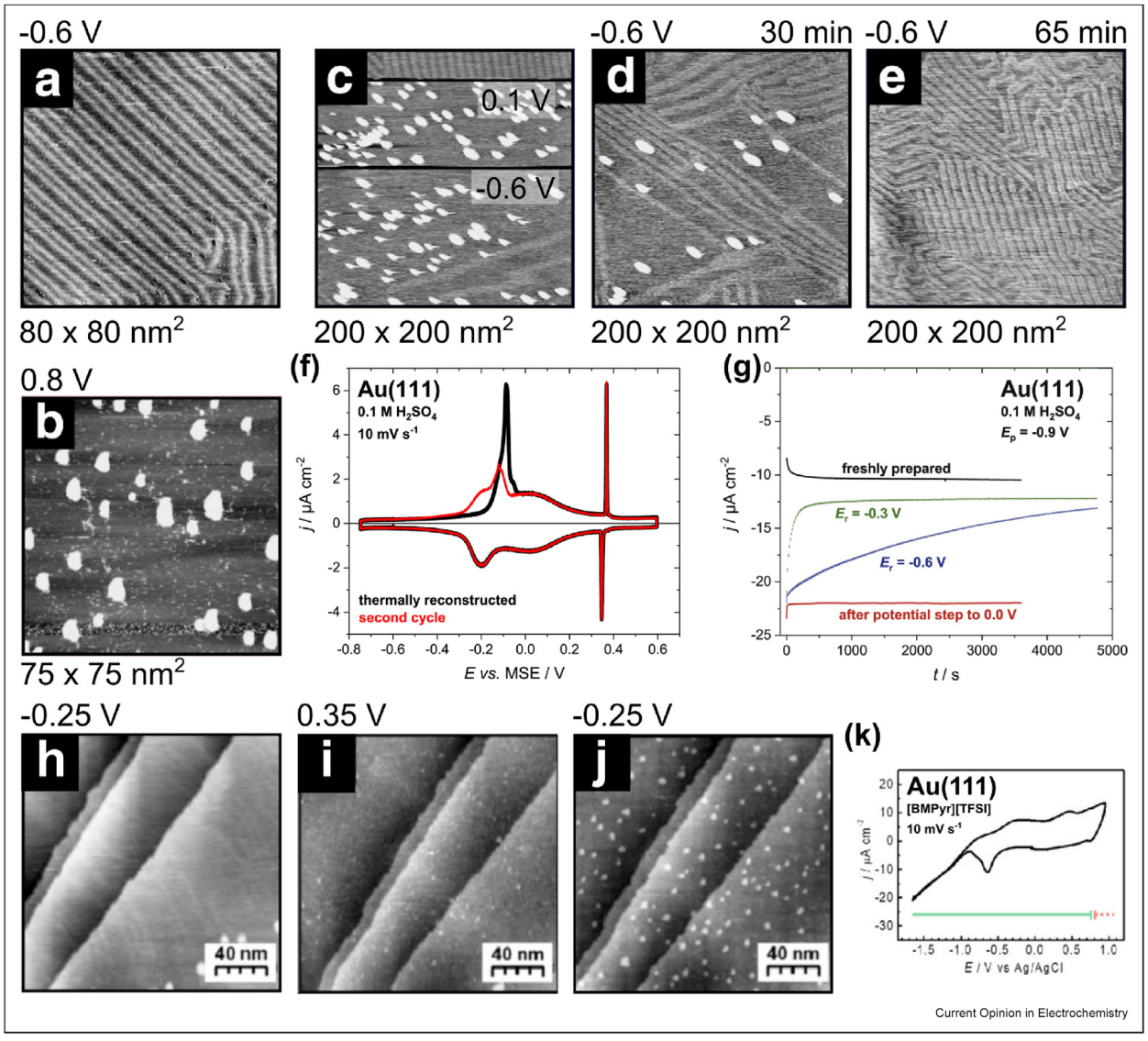

(a–g) *In situ* STM images of Au(111) electrode in 0.1 M H_2SO_4 [20]: **(a)** Thermally induced surface reconstruction at –0.6 V *versus* MSE and **(b)** Au(111) surface after the potential-induced lifting of the reconstruction at 0.8 V. **(c)** Potential steps from –0.9 V to –0.1 V and –0.6 V, and **(d and e)** subsequent formation of the herringbone reconstruction at –0.6 V. In **(f)** and **(g)**, the corresponding CVs and chronoamperometric plots are shown [21]. **(h–k)** *In situ* STM images of Au(111) in [BMPyr][TFSI] at **(h)** –0.25 V, **(i)** 0.35 V, and **(j)** –0.25 V *versus* Ag/AgCl after applying potentials up to 0.75 V and **(k)** corresponding CV [7]. (Adapted from Refs. [20,21,7]).

adsorption of specific (bi)sulphate anions. This leads to a higher defect density and island formation as shown in Figure 2b [20]. The sequence of images in Figure 2c–e shows how the reconstruction is lifted and then reformed by first jumping to 0.1 V and then to −0.6 V versus MSE [20]. Over time, a potential-induced surface reconstruction is formed, leading to the development of a herringbone structure distinct from the one observed through thermal reconstruction [20]. The potential-induced reconstruction is less ordered than the thermally induced reconstruction, leading to deviations in the positive-going scan of CVs from the first cycle, which starts on the thermally reconstructed Au(111) surface, to the second cycle, as shown in Figure 2f [21].

Figure 2g shows chronoamperometric plots for the hydrogen evolution reaction (HER) at −0.9 V [21]. The differences in the activity of the surface depending on the surface morphology are obvious: The thermally reconstructed surface has the lowest number of defects and is, thus, the least active for the HER. If the reconstruction was lifted previously, the HER activity is highest [21]. The current densities observed along the potential step series at both −0.3 V and −0.6 V *versus* MSE exhibit a gradual decline in HER activity over time, indicating structural changes due to potential-induced reconstruction [21]. The decline in activity is notably more pronounced for the more positive potential. This observation aligns with *in situ* STM studies, which have demonstrated that at potentials approaching the point at which the reconstruction is lifting, the reconstruction rows manifest more rapidly within minutes [25].

Recently, *in situ* STM investigations have been directed towards new classes of nonaqueous electrolytes as well, namely, ILs and deep eutectic solvents (DESs). To fundamentally understand the processes at the electrode–IL/DES interface, *in situ* STM was used in both classes of electrolytes [7,26]. As the electrolyte significantly influences the surface atoms' mobility, the morphologies of the reconstructed and unreconstructed surfaces show a huge variety when using different electrolytes [7,26]. For instance, the structural changes of a Au(111) single-crystal surface in *N*-butyl-*N*-methylpyrrolidinium dicyanamide ([BMPyr][DCA]) and *N*-butyl-*N*-methylpyrrolidinium bis(trifluoromethane) sulfonimide ([BMPyr][TFSI]) were investigated using *in situ* STM [7]. Here, the STM investigations of Au(111) in [BMPyr][TFSI] reveal a stable surface with only few corrugation lines as in Figure 2h within the potential range from −0.25 V down to −1.75 V *versus* Ag/AgCl [7]. Furthermore, the surface is stable upon shifting to positive potentials up to 0.35 V as shown in Figure 2i [7]. Going to more positive potentials, the noise in the image increases, and upon shifting the potential back to −0.25 V, small islands, approximately 0.25 nm in height, appear on the terraces as shown in Figure 2h–j [7]. One possible explanation is that a small amount of Au dissolved during electrode polarisation at positive potentials, possibly from steps or areas outside the scanned region [7]. The small islands observed in Figure 2j could result from the redeposition of gold atoms upon returning the potential to −0.25 V [7]. Figure 2k shows the corresponding CV of the system [7]. The green bar indicates the potential region in which the surface was stable as determined by *in situ* STM [7]. In comparison, when Au(111) was polarised in [BMPyr][DCA] at negative potentials, a $(\sqrt{3} \times 22)$ surface reconstruction was induced. At −0.30 V *versus* Ag/AgCl, this reconstruction pattern became unclear, indicating the initial lifting of the reconstruction, which is complete at −0.20 V *versus* Ag/AgCl. Similarly, as in ILs, the formation and lifting of the reconstruction of Au(111) is highly dependent on the components the DES includes. In the Cl^--containing ethaline, it was shown that the surface mobility was very high, so that the islands formed upon lifting the reconstruction were unstable [26]. The surplus of Au atoms diffused to the step edges within seconds [26].

Ordered ion adsorption

As specifically or nonspecifically adsorbed electrolyte molecules can be rather mobile on an electrode surface, in most *in situ* STM images, the electrode is imaged, while the electrolyte close to the electrode only contributes to the noise [27]. However, if the electrolyte's molecules form ordered adlayers, they are accessible by *in situ* STM. This can be achieved in different kinds of electrolytes as long as ordered adlayers exist. Figure 3 shows three examples for ordered adlayers on Au(111) in (a) acetic acid, (b) the IL [BMPyr][DCA], and (c) the DES ethaline (ethylene glycol:choline chloride 2:1) [6,7,26]. The investigation of such structures helps to understand the reactivity of the electrode at the respective potential because adsorbed layers can either block the surface for electrocatalytic reactions or promote these reactions [14,28]. Sometimes, differently ordered adlayers can even co-exist on the surface, as for instance, the $(\sqrt{3} \times \sqrt{3})$R23.45° and the (2×2) structures of acetate on Au(111) [6]. Nevertheless, after some time, only the (2×2) structure remains as thermodynamically stable configuration, since the $(\sqrt{3} \times \sqrt{3})$R23.45° structure is metastable [6]. For the [BMPyr][TFSI] adsorption $(\sqrt{7} \times \sqrt{7})$R19.1° structures of two different species were found, which could be related to the cations or anions [7]. Both the anions and cations seem to alternate on the surface at the respective potential [7]. In the DES ethaline, the chloride anions form a $(\sqrt{3} \times \sqrt{3})$R30° adlayer [26].

Metal deposition

Metal electrodeposition plays a pivotal role for a variety of applications. For instance, in the field of

Figure 3

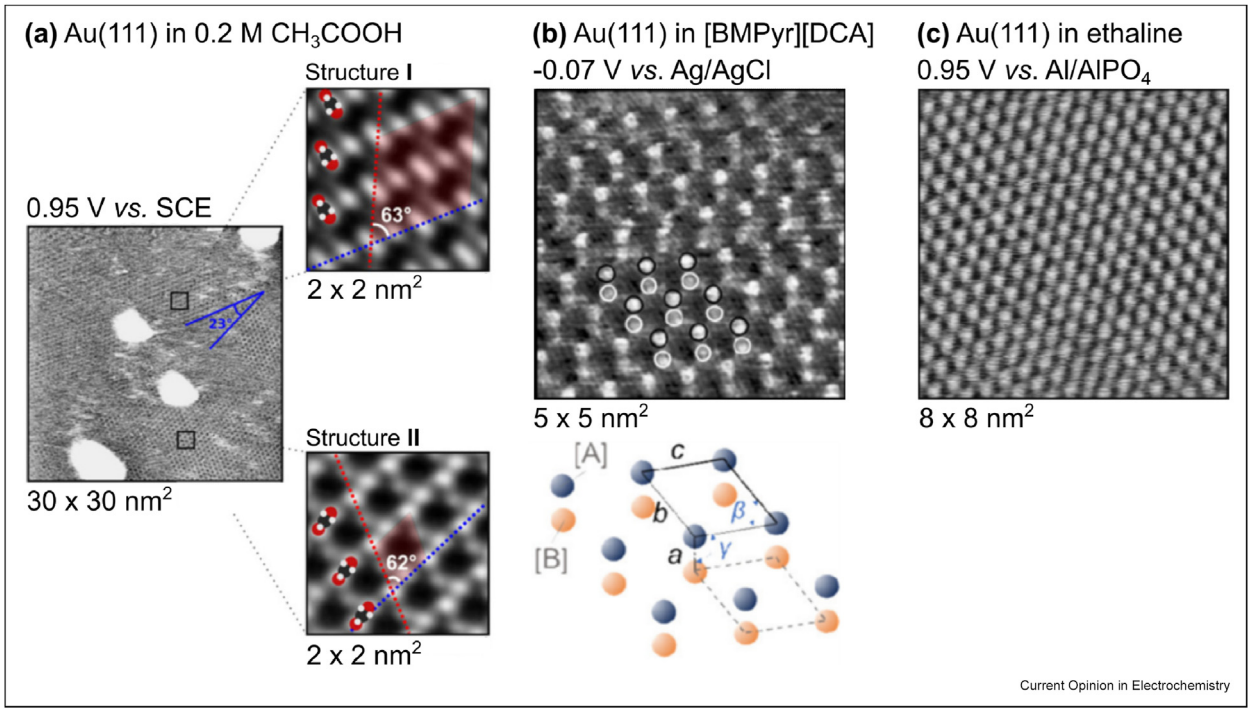

In situ STM image of ordered adsorbate adlayers on Au (111) in **(a)** acetic acid [6], **(b)** [BMPyr][DCA] with a schematic illustration of the adsorbate arrangement of two different species [A] and [B] on the surface [7], and **(c)** ethaline as previous shown in Ref. [26] (Adapted from Refs. [6,7]).

electrochemical energy storage, it is a key factor in constructing stable metal batteries [30,31]. In addition, metal deposits on a foreign substrate can enhance the activity of an electrocatalyst [32]. In all these applications, controlling the morphology of the deposition is crucial. Here, *in situ*, STM can provide important insights into the initial stages of metal deposition and the resulting bulk morphologies. It also facilitates the investigation of processes such as dealloying [28,33].

Information about the potentials of underpotential deposition (UPD) and overpotential deposition (OPD) can already be extracted from pure electrochemical measurements, such as cyclic voltammetry or chronoamperometry. Nevertheless, no information about the actual active sites or the morphology of the deposited material can be extracted from these measurements. However, this information is accessible by *in situ* STM measurements. For example, the initial stages and ongoing UPD of Na deposition on a Au(111) from the IL *N*-methyl-*N*-propylpiperidinium bis(trifluoromethane)sulfonimide ([MPPip][TFSI]) were investigated in Figure 4 [29]. The images a–c show the first nucleation on the Au(111) electrode. At 1.3 V *versus* Na/Na^+, the deposition has not yet started, and the bare herringbone reconstructed Au (111) surface is visible in Figure 4a [29]. Decreasing the potential to 1.1 V as shown in Figure 4b, small islands have nucleated at the so-called elbow sites of the herringbone reconstruction [29]. These islands are not imaged with monoatomic height, either due to the chemical contrast or due to an insertion of the deposited atoms in the substrate [29]. After a further potential decrease to 1.0 V, islands of monoatomic height started to nucleate at the elbow sites [29]. Similar preferential deposition was also observed for the deposition of other metals, such as Co or Ni [34,35].

The images in Figure 4e–g show the ongoing UPD and were all recorded at 0.5 V [29]. Whereas in the CVs shown in Figure 4d, only one broad peak in this potential region was seen, the *in situ* STM images reveal that three processes occur subsequently [29]. First, the islands grow, and more islands nucleate. Then, these islands coalesce into layers before a three-dimensional growth starts and a cauliflower-like structure evolves. These details cannot be extracted from pure electrochemical measurements [29].

Of course, the composition of the electrolyte, the used substrate, and the substrate's orientation greatly influence the deposited metal's morphology, as shown by several *in situ* STM studies in which different metals were deposited [35–38].

Figure 4

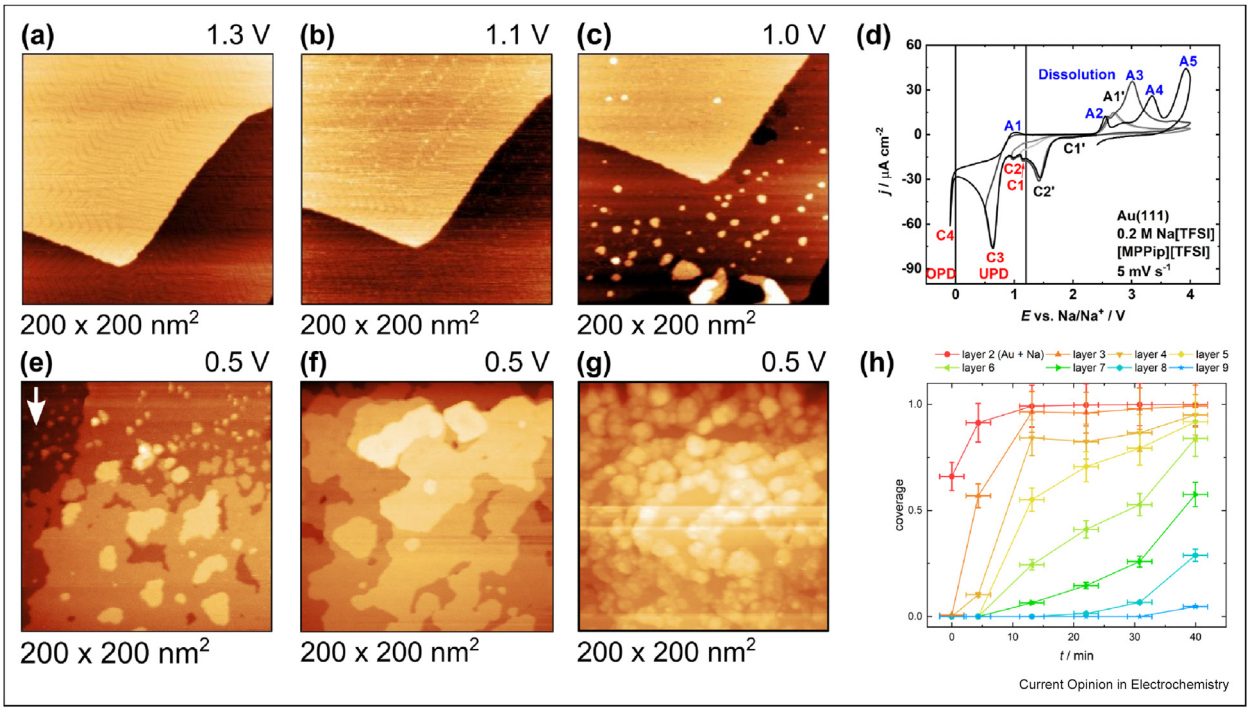

Na deposition form the IL [MPPip][TFIS] on Au(111) [29]: **(a–c)** *In situ* STM images of the initial island growth at the elbow sites of the reconstruction lines. **(d)** CVs of the system, **(e,f)** ongoing UPD from island growth to layer coalescence and three-dimensional growth, **(h)** monolayer coverage determined from the STM measurements (adapted from Ref. [29].)

As long as no side reactions occur, the amount of electrodeposited material can be determined by the charge transferred during electrodeposition [28,39]. *In situ* STM allows us to determine the local coverage of the deposited material even if electrochemical side reactions co-occur. This is, for example, relevant in ILs, where side processes of residual impurities often contribute to Faradaic currents. Exemplarily, Figure 4h shows the coverage of each layer extracted from the series of *in situ* STM measurements shown in Figures 4e–g [29].

As for the metal deposition, a quantitative analysis of the metal dissolution can be conducted by *in situ* STM measurements. For example, the dealloying of Cu from Au after the overpotential deposition of Cu on a Au(111) surface was observed this way [28]. This phenomenon is not accompanied by huge currents because it is a rather slow process. However, *in situ* STM measurements still allow us to quantify the number of layers dissolved per time [28].

Conclusion

In situ STM is a very powerful technique in many fields of electrochemistry, with the unique ability to provide detailed insights into the structure and dynamics of the electrode–electrolyte interface. By combining electrochemical measurements with STM, measured currents can be related to morphological changes at the interface. This helps in understanding phenomena such as electrocatalytic reactions, metal deposition and dissolution, surface oxidation, or even corrosion. While *in situ* STM measurements are not capable to provide chemical information, these could be obtained by combination with additional *ex situ* surface science techniques, such as X-ray photo-electron spectroscopy or Auger electron spectroscopy. With the increasing development and use of artificial intelligence on scanning probe techniques and in data evaluation, it can be expected that *in situ* STM measurements can be facilitated in the future.

CRediT

M.-K. Heubach: Conceptualization, Visualization, Supervision, Writing – original draft preparation, Data curation. **Y. Mattausch**: Visualization, Writing – original draft preparation. **T. Jacob**: Writing – review & editing, Resources, Funding acquisition.

Declaration of competing interest

The authors declare that they have no known competing financial interests or personal relationships that could have appeared to influence the work reported in this paper.

Data availability

Data will be made available on request.

Acknowledgements

This work was funded by the Deutsche Forschungsgemeinschaft (DFG, German Research Foundation) under Germany's Excellence Strategy – EXC 2154 – Project number 390874152. Furthermore, the authors gratefully acknowledge funding by the DFG through project 501805371 as well as by the BMBF (Bundesministerium fur Bildung und Forschung) through the project CASINO (FKZ: 03XP0487G) and the state of Baden-Württemberg and the DFG through grant no INST 40/574-1 FUGG.

References

Papers of particular interest, published within the period of review, have been highlighted as:

- • of special interest
- •• of outstanding interest

1. Binnig G, Rohrer H, Gerber C, Weibel E: **Surface studies by scanning tunneling microscopy**. *Phys Rev Lett* 1982, **49**: 57–61, https://doi.org/10.1103/PhysRevLett.49.57.

2. Itaya K, Tomita E: **Scanning tunneling microscope for electrochemistry - a new concept for the in situ scanning tunneling microscope in electrolyte solutions**. *Surf Sci* 1988, **201**:L507–L512, https://doi.org/10.1016/0039-6028(88)90489-X.

3. •• Liang Y, Pfisterer JHK, McLaughlin D, Csoklich C, Seidl L, Bandarenka AS, Schneider O: **Electrochemical scanning probe microscopies in electrocatalysis**. *Small Methods* 2019, **3**, 1800387, https://doi.org/10.1002/smtd.201800387.
Conclusive overview on electrochemical scanning probe methods.

4. Schneeweiss MA, Kolb D: **Das rastertunnelmikroskop in der elektrochemie**. *Chem Unserer Zeit* 2000, **34**:72–83, https://doi.org/10.1002/1521-3781(200004)34:2¡72::AID-CIUZ72¿3.0.CO;2-5.

5. Schuett FM, Zeller S, Matzik FM, Heubach M-K, Geng T, Hermann JM, Uhl M, Kibler LA, Engstfeld AK, Jacob T: **Versatile 3d-printed micro-reference electrodes for aqueous and non-aqueous solutions**. *Angew Chem Int Ed* 2021, **133**: 22783–22790, https://doi.org/10.1002/anie.202105871.

6. Abdelrahman A, Hermann JM, Jacob T, Kibler LA: **Adsorption of acetate on au(111): An in-situ scanning tunnelling microscopy study and implications on formic acid electrooxidation**. *ChemPhysChem* 2019, **20**:2989–2996, https://doi.org/10.1002/cphc.201900560.

7. Rudnev AV, Ehrenburg MR, Molodkina EB, Abdelrahman A, Arenz M, Broekmann P, Jacob T: **Structural changes of au(111) single-crystal electrode surface in ionic liquids**. *Chemelectrochem* 2020, **7**:501–508, https://doi.org/10.1002/celc.201902010.

8. • Schwarz UD, Haefke H, Reimann P, Güntherodt H: **Tip artefacts in scanning force microscopy**. *J Microsc* 1994, **173**:183–197, https://doi.org/10.1111/j.1365-2818.1994.tb03441.x.
Conclusive overview on several tip effects occurring in scanning probe microscopy measurements.

9. Pelz JP, Koch RH: **Tip-related artifacts in scanning tunneling potentiometry**. *Phys Rev B* 1990, **41**:1212–1215, https://doi.org/10.1103/PhysRevB.41.1212.

10. Kolb DM, Simeone FC: *Characterization and modification of electrode surfaces by in situ STM*. Wiley; 2009:119–146, https://doi.org/10.1002/9783527628827.ch5.

11. Alsabet M, Grden M, Jerkiewicz G: **Electrochemical growth of surface oxides on nickel. part 1: formation of α-ni (oh) 2 in relation to the polarization potential, polarization time, and temperature**. *Electrocatalysis* 2011, **2**:317–330.

12. Shields SS, Gupta JA: **Stm study of surface restructuring of oxidized cu (100)**. *Surf Sci* 2024, **740**, 122403.

13. Griesser C, Winkler D, Moser T, Haug L, Thaler M, Portenkirchner E, Klötzer B, Diaz-Coello S, Pastor E, KunzeLiebhäuser J: **Lab-based electrochemical x-ray photoelectron spectroscopy for in-situ probing of redox processes at the electrified solid/liquid interface**. *Electrochemical Sci Adv* 2023, e2300007, https://doi.org/10.1002/elsa.202300007.

14. • Maurice V, Marcus P: **Application of surface science to corrosion**. *Surf Interf Sci: Volume 10: Appl of Surf Sci II* 2020, **10**: 799–825.
Conclusive overview on application of *in situ* STM to corrosion.

15. • Hersbach TJ, Koper MT: **Cathodic corrosion: 21st century insights into a 19th century phenomenon**. *Curr Opin Electrochem* 2021, **26**, 100653, https://doi.org/10.1016/j.coelec.2020.100653.
Conclusive overview on the cathodic corrosion of Pt.

16. • Elnagar MM, Hermann JM, Jacob T, Kibler LA: **Tailoring the electrode surface structure by cathodic corrosion in alkali metal hydroxide solution: Nanostructuring and faceting of au**. *Curr Opin Electrochem* 2021, **27**, 100696, https://doi.org/10.1016/j.coelec.2021.100696.
Conclusive overview on the cathodic corrosion of Au.

17. Liu Z, Höfft O, Gödde AS, Endres F: **In situ electrochemical xps monitoring of the formation of anionic gold species by cathodic corrosion of a gold electrode in an ionic liquid**. *J Phys Chem C* 2021, **125**:26793–26800, https://doi.org/10.1021/acs.jpcc.1c07450.

18. Heubach M-K, Schuett FM, Abdelrahman A, Kibler LA, Jacob T: **Au (111) in [mppip][tfsi] in dependence of water content: revealing the initial stages of cathodic corrosion using in-situ stm**. In *Electrochemical society meeting abstracts 241, 16, the electrochemical society*. Inc.; 2022. 988–988.

19. Li H, Liang Y, Ju W, Schneider O, Stimming U: **In situ monitoring of the surface evolution of a silver electrode from polycrystalline to well-defined structures**. *Langmuir* 2022, **38**: 14981–14987.

20. Kibler LA, Hermann JM, Abdelrahman A, El-Aziz AA, Jacob T: **New insights on hydrogen evolution at au single crystal electrodes**. *Curr Opin Electrochem* 2018, **9**:265–270, https://doi.org/10.1016/j.coelec.2018.05.013.

21. Hermann JM, Abdelrahman A, Jacob T, Kibler LA: **Potential-dependent reconstruction kinetics probed by her on au(111) electrodes**. *Electrochim Acta* 2020, **347**, 136287.

22. Kolb D: **Reconstruction phenomena at metal-electrolyte interfaces**. *Prog Surf Sci* 1996, **51**:109–173, https://doi.org/10.1016/0079-6816(96)00002-0.

23. Dakkouri A, Kolb D: *Reconstruction of gold surfaces*. New York: Marcel Dekker; 1999:151–173.

24. Ibach H. *Physics of surfaces and interfaces*, **1**. Springer; 2006, https://doi.org/10.1007/3-540-34710-0.

25. He Y, Borguet E: **Metastable phase of the au (111) surface in electrolyte revealed by stm and asymmetric potential pulse perturbation**. *J Phys Chem C* 2011, **115**:5726–5731, https://doi.org/10.1021/jp110484w.

26. Tan Z, Peng Y, Liu J, Yang Y, Zhang Z, Chen Z, Mao B, Yan J: **An in situ scanning tunneling microscopy study on the electrochemical interface between au(111) and ethaline deep eutectic solvent**. *Chemelectrochem* 2020, **7**:4601–4605, https://doi.org/10.1002/celc.202001264.

27. Haid RW, Kluge RM, Liang Y, Bandarenka AS: **In situ quantification of the local electrocatalytic activity via electrochemical scanning tunneling microscopy**. *Small Methods* 2021, **5**, 2000710, https://doi.org/10.1002/smtd.202000710.

28. Fackler S, Wittmann M, Heubach M, Hermann J, Kibler L, Jacob T: **Underpotential deposition of cu onto au(111) in the presence of acetate**. *Electrochim Acta* 2024, **490**, 144225, https://doi.org/10.1016/j.electacta.2024.144225.

29. Heubach M, Schuett FM, Kibler LA, Abdelrahman A, Jacob T: **Initial stages of sodium deposition onto au(111) from [mppip][tfsi]: An in-situ stm study for sodium-ion battery electrolytes**. *Chemelectrochem* 2022, **9**, e202200722, https://doi.org/10.1002/celc.202200722.

30. Jana A, García RE: **Lithium dendrite growth mechanisms in liquid electrolytes**. *Nano Energy* 2017, **41**:552–565, https://doi.org/10.1016/j.nanoen.2017.08.056.

31. Berger CA, Ceblin MU, Jacob T: **Lithium deposition from a piperidinium–based ionic liquid: rapping dendrites on the knuckles**. *Chemelectrochem* 2017, **4**:261–265, https://doi.org/10.1002/celc.201600730.

32. Auer A, Sarabia FJ, Winkler D, Griesser C, Climent V, Feliu JM, Kunze-Liebhäuser J: **Interfacial water structure as a descriptor for its electro-reduction on ni (oh) 2-modified cu (111)**. *ACS Catal* 2021, **11**:10324–10332.

33. Chen S, Sanz F, Ogletree D, Hallmark V, Devine T, Salmeron M: **Selective dissolution of copper from au-rich cu-au alloys: an electro chemical stm study**. *Surf Sci* 1993, **292**:289–297, https://doi.org/10.1016/0039-6028(93)90334-G.

34. Möller FA, Magnussen OM, Behm RJ: **Overpotential-controlled nucleation of ni island arrays on reconstructed au(111) electrode surfaces**. *Phys Rev Lett* 1996, **77**:5249–5252, https://doi.org/10.1103/PhysRevLett.77.5249.

35. Kleinert M, Waibel HF, Engelmann GE, Martin H, Kolb DM: **Co deposition on au(111) and au(100) electrodes: An in situ stm study**. *Electrochim Acta* 2001, **46**:3129–3136, https://doi.org/10.1016/S0013-4686(01)00604-1.

36. Schuett FM, Heubach M-K, Mayer J, Ceblin MU, Kibler LA, Jacob T: **Electrodeposition of zinc onto au(111) and au(100) from the ionic liquid [mppip][tfsi]**. *Angew Chem Int Ed* 2021, **60**:20461–20468, https://doi.org/10.1002/anie.202107195.

37. Herrero E, Buller LJ, Abruña HD: **Underpotential deposition at single crystal surfaces of au, pt, ag and other materials**. *Chem Rev* 2001, **101**:1897–1930.

38. Cagnon L, Gundel A, Devolder T, Morrone A, Chappert C, Schmidt J, Allongue P: **Anion effect in co/au (111) electrodeposition: structure and magnetic behavior**. *Appl Surf Sci* 2000, **164**:22–28.

39. Zhang J, Sung Y-E, Rikvold PA, Wieckowski A: **Underpotential deposition of cu on au (111) in sulfate-containing electrolytes: A theoretical and experimental study**. *J Chem Phys* 1996, **104**:5699–5712.